Chemical Science

ROYAL SOCIETY OF CHEMISTRY

EDGE ARTICLE

View Article Online
View Journal | View Issue

Cite this: *Chem. Sci.*, 2025, **16**, 9169

All publication charges for this article have been paid for by the Royal Society of Chemistry

Tuning intramolecular charge transfer and suppressing rotations in thianthrene derivatives for enhancement of room-temperature phosphorescence†

Huiwen Zeng,[a] Hualiu Li,[a] Peng Zhen,[a] Jiadong Zhou,*[a] Bingjia Xu,*[b] Guang Shi,[a] Yujian Zhang,[c] Zhenguo Chi[b] and Cong Liu*[a]

Polymer-based organic room-temperature phosphorescent (ORTP) materials have advantages such as low cost, abundant resources and ease of processing, rendering them highly suitable for real-world applications. However, the trade-off between the phosphorescence quantum yield ($\Phi_{phos.}$) and phosphorescence lifetime ($\tau_{phos.}$) highlights the challenge for the development of efficient ORTP materials. Here, a synergistic strategy was proposed to promote n–π* transitions, provide charge-transfer (CT) intermediate and inhibit intramolecular motions to achieve efficient ORTP. A thianthrene (TA) unit was attached to planar and rigid polyaromatic hydrocarbons (PAHs), and the resulting luminogens were used as guest molecules and embedded into melamine-formaldehyde (MF) polymers, respectively. The TA chromophore promotes n–π* transitions, and the PAH units generate CT intermediates and inhibit rotations, which open intersystem crossing (ISC) channels and facilitate ISC processes. It was found that the $\tau_{phos.}$ values of TA-Na@MF and TA-Phen@MF were about 30-fold that of TA@MF. The phenanthryl group was larger than the naphthyl group, which created steric hindrance and limited rotations. As a result, TA-Phen@MF demonstrated the best RTP performance with an ultralong $\tau_{phos.}$ of 1006.45 ms and a high $\Phi_{phos.}$ of 50.31%. To the best of our knowledge, the observed RTP represents the longest persistence luminescence among TA derivatives. Thanks to its efficient RTP properties and processability, TA-Phen@MF was blended with ethylene vinyl acetate (EVA) to produce stretchable and recyclable persistent RTP elastomers. This work provides helpful guidance for achieving high-performance polymer-based ORTP materials.

Received 14th February 2025
Accepted 18th April 2025

DOI: 10.1039/d5sc01176k

rsc.li/chemical-science

Introduction

Organic room-temperature phosphorescent (ORTP) materials have attracted widespread attention owing to their unique characteristics and also their special advantages in the fields of optoelectronic biotechnological applications such as bio-imaging,[1–3] information encryption[4–6] and sensing.[7,8] Indeed, ORTP materials represent a class of luminescent materials with rich molecular diversity, easily modifiable structures and good biocompatibility.[9–11] However, achieving purely organic materials with high phosphorescence quantum yield ($\Phi_{phos.}$) and ultralong lifetime ($\tau_{phos.}$) under ambient conditions remains challenging due to the intrinsic spin-forbidden transition between singlet and triplet excited states of organic molecules and the fast nonradiative decay of triplet excitons.[12,13] Therefore, increasing the spin–orbit coupling (SOC), promoting the intersystem crossing (ISC) rate, and improving the triplet exciton stability of organic molecules are crucial for achieving efficient RTP.[14–17] In molecular design, one typical method to generate efficient ORTP emission is to introduce halogen atoms with heavy-atom effects (Cl, Br, and I) or heteroatoms with lone pair electrons (O, N, S, and P) to facilitate ISC from singlet to triplet excited states.[18–20] Additionally, forming aggregates with more stable triplet excited states through intermolecular π–π stacking can effectively extend RTP lifetimes. However, it is challenging to develop high-performance ORTP materials since the long $\tau_{phos.}$ and high $\Phi_{phos.}$ conflict in principle.[21–23] For example, efficient ISC will enhance the phosphorescence radiative rate, which usually reduces the $\tau_{phos.}$. Achieving high-performance ORTP materials still lacks clear design principles.

Thianthrene (TA) is an organic molecule with a folding conformation, and most of its derivatives exhibit RTP emission under vacuum conditions because of the folding-induced SOC enhancement.[24–26] Many strategies were proposed to achieve

[a]School of Chemistry, South China Normal University, Guangzhou 510006, PR China. E-mail: liucong_011@163.com

[b]School of Environmental and Chemical Engineering, Wuyi University, Jiangmen 529020, PR China

[c]School of Chemistry, Zhejiang Normal University, Jinhua 321004, PR China

† Electronic supplementary information (ESI) available. CCDC 2411623–2411625 and 2411637. For ESI and crystallographic data in CIF or other electronic format see DOI: https://doi.org/10.1039/d5sc01176k

highly efficient organic RTP materials based on the TA unit by tuning their folding geometries, modifying the π-conjugations, and combining functional units.[27–29] In 2022, Yang's group chemically modified TA into intramolecular dimers to enhance the RTP properties. Dual-emission of fluorescence and phosphorescence was shown when dispersing these dimers in a PMMA matrix, with the highest RTP quantum yield of 40.7% and an RTP lifetime of 36.5 ms in a vacuum.[30] In 2023, Yang's group combined TA-like folding units with various luminescent cores to achieve a series of RTP materials with tunable colors, among which the maximum RTP quantum yield was 43.58%, but the RTP lifetime was only 12.9 ms in a vacuum.[31] In 2024, Li's group engineered three TA derivatives by modifying the π-conjugation, creating a PMMA-doped system that demonstrated thermally erasable photochromism with an RTP lifetime of 431.78 ms and a photoluminescence quantum yield of 1.95% in a vacuum.[32] It can be seen that the performance of TA-based organic RTP materials is still not satisfactory due to the lack of universal molecular design strategies (Tables S1 and S2†). As a result, molecular design strategies for achieving high $\Phi_{phos.}$ and ultralong $\tau_{phos.}$ TA-based RTP materials are highly desirable.

In addition, triplet excitons are prone to deactivation through molecular non-radiative vibrations and quenching by oxygen and water molecules, leading to decreased ORTP efficiency.[33–35] Crystal engineering,[36–38] host–guest doping,[39–41] polymer doping[42–44] and copolymerization[45–47] can provide an external rigid environment to restrict intramolecular motions and isolate moisture and oxygen for stabilizing triplet excitons, thereby achieving efficient ORTP.[48–50] In contrast, polymer-based RTP materials have attracted increasing interest due to their ease of processing and flexibility.[51–53] In this context, some small molecules were doped into polymer matrices, for example, conventional poly(methyl methacrylate) (PMMA) and polyvinyl alcohol (PVA), but their stretchability was poor. It is crucial to develop new polymer matrices for doping systems to meet different applications.

In this work, a series of TA derivatives was synthesized by linking phenyl, naphthyl and phenanthryl groups at the *a* position of the TA unit, and then they were embedded into melamine-formaldehyde (MF) polymers with permanent and compact three-dimensional (3D) networks to achieve ORTP materials with both a high $\Phi_{phos.}$ and an ultralong $\tau_{phos.}$. Herein, TA was employed as the essential chromophore, owing to its unique folding-induced SOC enhancement properties, which is in favor of facilitating ISC processes to produce triplet excitons. In the meantime, polyaromatic hydrocarbons (PAHs), which have planar and rigid chemical structures, were selected as substituents to inhibit the intramolecular motions to reduce non-radiative decay channels.[54–57] It was found that the TA-doped MF polymer showed a significant green RTP emission but with a limited lifetime of 30.39 ms. However, when introducing the naphthyl and phenanthryl groups, the lifetimes of the resulting materials based on TA-Na and TA-Phen luminogens extended about 30 times. For TA-Phen@MF materials, their $\Phi_{phos.}$ and $\tau_{phos.}$ were up to 50.31% and 1006.45 ms under ambient conditions, respectively. To the best of our knowledge, the observed RTP represents the longest persistence luminescence among the TA derivative family (Tables S1 and S2†). Theoretical calculations indicated that the TA derivatives probably form charge transfer (CT) states, enabling highly efficient ISC for the production of long-lived triplet excitons. Thanks to its processability, the TA-Phen@MF RTP material was solution blended with ethylene vinyl acetate (EVA) matrices to produce stretchable and flexible elastomer materials with stable persistent luminescence properties. This work not only provides helpful guidance for creating high-performance polymer-based ORTP materials but also demonstrates a simple and effective strategy for obtaining RTP elastomers.

Results and discussion

The TA derivatives were facilely synthesized by linking a phenyl, naphthyl, or phenanthryl group at the *a* position of TA through the Suzuki coupling reaction (Scheme S1†), respectively. The target compounds were purified *via* silica gel column chromatography and/or recrystallization. Their chemical structures were fully characterized by nuclear magnetic resonance spectroscopy (^{1}H NMR and ^{13}C NMR), high-resolution mass spectrometry, and single-crystal X-ray diffraction (Fig. S14–S25†).

As shown in Fig. S1,† in dilute 2-methyltetrahydrofuran (2-MeTHF) solutions, all the TA derivatives exhibited a similar UV-visible absorption band that peaked at about 270 nm and steady-state fluorescence band that peaked at about 320 nm, which was ascribed to the n–π* transition of the TA fragment. Notably, when the temperature was 77 K, the glassy solutions exhibited an obvious green afterglow (Fig. S2a†). The delayed photoluminescence (PL) spectra showed a similar (phosphorescent) shape that peaked at about 485–520 nm for the reference TA and the three TA derivatives. The phosphorescence lifetime of TA was 445.09 ms, while it reached 576.50 ms for TA-Ph, 858.82 ms for TA-Na and 1332.79 ms for TA-Phen in 2-MeTHF solution at 77 K (Fig. S2b†). That is, the introduction of PAH groups did not influence the vertical electronic processes, which originated from the local excitation of the TA fragment. Moreover, the phosphorescent properties were observed at cryogenic temperature, and the PAH groups contributed to the enhancement of phosphorescence lifetimes.

To activate their RTP properties, the reference TA and the three TA derivatives were dispersed into the dense 3D crosslinked MF matrix with variable doping concentrations. The doped films were prepared by mixing a homogeneous THF mixture of TA or TA derivatives (6 mg mL^{-1}) with an MF pre-polymer (60%, 1 g) at 150 °C for 10 minutes, followed by hot-pressing using a mold. Since the thermal decomposition temperatures (T_d) of TA, TA-Ph, TA-Na, and TA-Phen at a weight loss of 5% all exceed 160 °C, there would be no decomposition during the processing of MF (Fig. S3†). With an increase in the dopant concentration, the delayed emission intensity of the MF-doped films reaching a maximum at 1.00%, 1.00%, 0.50% and 0.10% corresponded to TA, TA-Ph, TA-Na and TA-Phen (Fig. S4 and S5†); they also have a comparatively longer phosphorescence lifetime (Fig. S6†). Therefore, the MF films of TA, TA-Ph, TA-Na and TA-Phen corresponding to dopant concentrations of 1.00%, 1.00%, 0.50% and 0.10% (hereafter denoted as TA@MF, TA-Ph@MF, TA-Na@MF and TA-Phen@MF) were selected as models to further investigate their photophysical properties. On the other hand, the

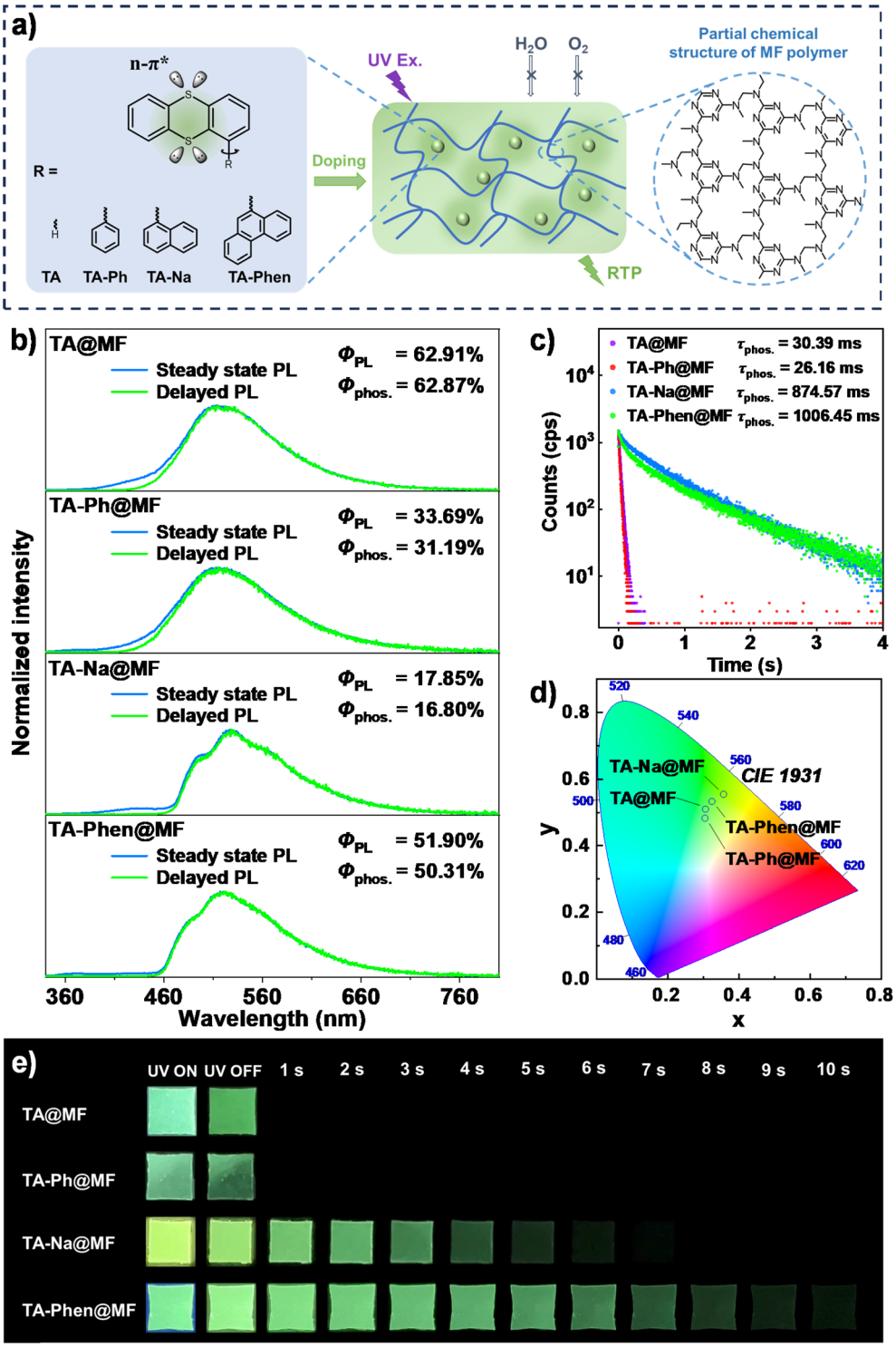

Fig. 1 (a) Chemical structures of thianthrene and its derivatives and the schematic diagram of small molecules doped in an MF polymer with a 3D covalent network. (b) The steady-state PL spectra and the delayed emission spectra (delayed 1 ms) of TA@MF, TA-Ph@MF, TA-Na@MF and TA-Phen@MF (excitation: 300 nm). (c) The delayed emission decay curves and lifetimes of TA@MF, TA-Ph@MF, TA-Na@MF and TA-Phen@MF (excitation: 300 nm). (d) The $CIE_{x,y}$ chromaticity coordinates of the persistent luminescence of TA@MF, TA-Ph@MF, TA-Na@MF and TA-Phen@MF. (e) Afterglow images of TA@MF, TA-Ph@MF, TA-Na@MF and TA-Phen@MF (excitation: 300 nm).

wavelength of the maximum emission peak remained unchanged for the MF films as the doping concentration and excitation wavelength changed, indicating that the phosphorescence of the films probably came from single molecules (Fig. S4, S5 and S7†).

As shown in Fig. 1b and S2,† all the doped polymer films exhibited similar delayed emission spectra and peaked at about 520 nm, which were little red shift compared with the ones in 2-MeTHF solutions at 77 K. The steady-state PL spectra almost

overlapped with their delayed spectra, indicating highly efficient ISC processes and pure RTP properties for the guest molecules doped in MF polymer films. The $\Phi_{phos.}$ values were 62.87%, 31.19%, 16.80% and 50.31% for TA@MF, TA-Ph@MF, TA-Na@MF and TA-Phen@MF (Fig. 1b), respectively, and the corresponding $\tau_{phos.}$ values were 30.39, 26.16, 874.57 and 1006.45 ms (Fig. 1c). Compared with the original TA@MF, the $\tau_{phos.}$ of TA-Na@MF and TA-Phen@MF increased significantly, attributed to the introduction of naphthyl and phenanthryl groups. In particular, the $\tau_{phos.}$ of TA-Phen@MF was enhanced over 30 times and remained at a comparable phosphorescence quantum yield. In addition, when these guest luminogens were doped into PMMA, the $\tau_{phos.}$ of TA-Phen@PMMA was also enhanced over 30 times when compared with that of TA@PMMA, but shorter than that of TA-Phen@MF (Fig. S8 and S9†). So, the long lifetime of these materials is also related to the compact 3D covalent network of the MF materials. The $\tau_{phos.}$ of TA-Phen@MF showed the longest lifetime persistent ORTP materials based on the TA family to date (Table S2†). To the best of our knowledge, among polymer-based ORTP materials with a lifetime above 1 second, TA-Phen@MF exhibits outstanding $\Phi_{phos.}$ (Tables S3 and S4†). The doped films presented green luminescence (Fig. 1d). The bright green luminescence persisted for many seconds even after the UV light was turned off, and the persistent luminescence lasted up to 10 s for TA-Phen@MF (Fig. 1e). When the temperature was up to 150 °C, TA-Na@MF and TA-Phen@MF still showed RTP performance, with lifetimes as long as 173.36 ms and 136.54 ms, respectively, demonstrating excellent high-temperature phosphorescence properties (Fig. S10 and S11†).

Single crystal structures of these four compounds were produced since the ISC processes and RTP properties have a close relationship with molecular conformation (Table S5†). As shown in Fig. 2a, the TA fragments in these molecules have folded angles between 122° and 135°, which will enhance the SOC by the folding-induced SOC enhancement mechanism.[24–26] Notably, the PAH substituent caused stereoisomerism in the TA derivatives owing to the folding orientation of the TA fragment. On the other hand, the single C–C bonding causes rotation motions, which imply various molecular conformations. TA-Ph molecules exhibit two enantiomers with similar conformational geometries, in which the torsion angles between TA and phenyl

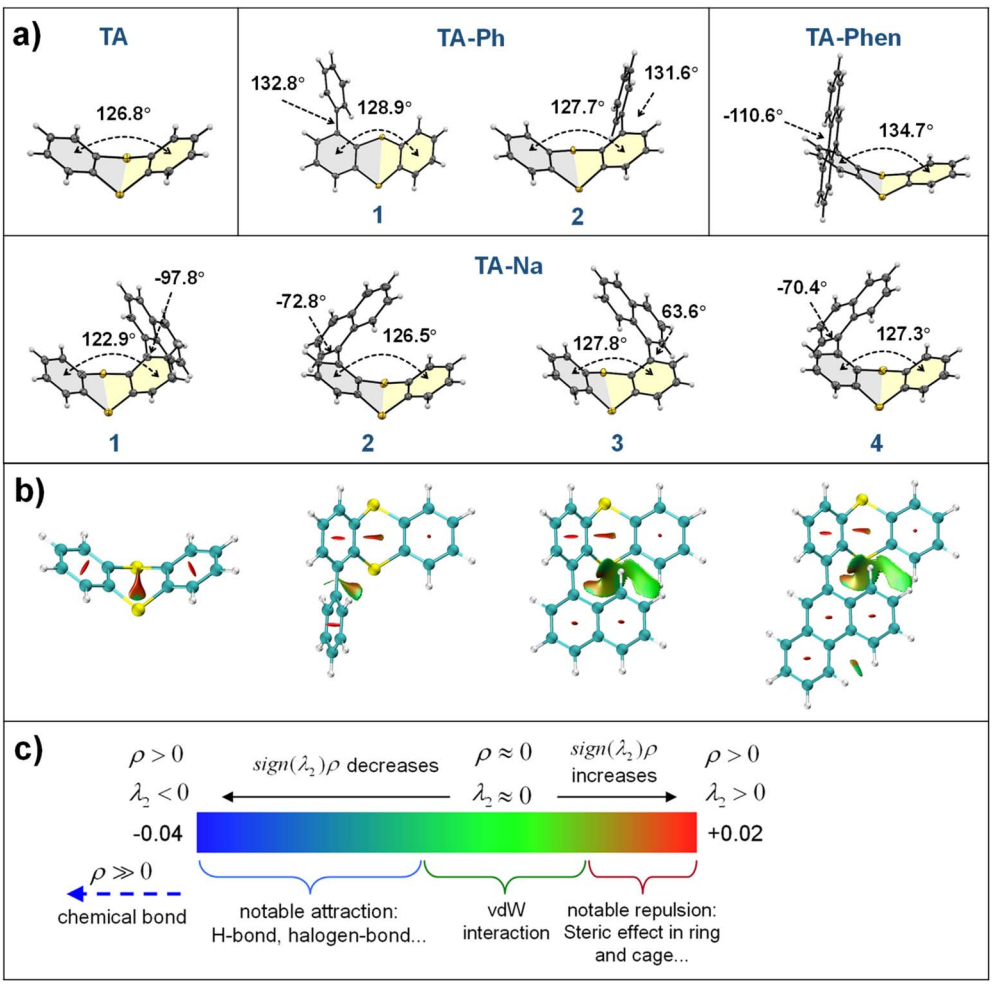

Fig. 2 (a) The molecular conformations of TA, TA-Ph, TA-Na and TA-Phen in single crystals. (b) The interaction region indicators (IRIs) of TA, TA-Ph, TA-Na, and TA-Phen. (c) IRI color bar corresponding to (b).

groups are 132.8° and 131.6°, respectively. The single crystal structures of TA-Na are more complex, and there are four independent conformations. Thereinto, a pair of enantiomers exhibit identical torsion angles of −70.4° and −72.8° between the TA and naphthyl groups, while two independent conformational geometries show torsion angles of 63.6° and −97.8°, respectively. The reduced $\Phi_{phos.}$ of TA-Ph@MF and TA-Na@MF, when compared to TA@MF, may be caused by intramolecular rotations between the TA and phenyl or naphthyl groups. However, there is only one independent conformation for TA-Phen in which the torsion angle is −110.6°. Therefore, the molecular rotation motions for TA derivatives are correlated with the number of fused rings for PAH units, of which the naphthyl group appears to be more sensitive. The non-covalent interaction (NCI) between the intramolecular fragments was reflected by the interaction region indicator (IRI).[58] As shown in Fig. 2b and c, the larger PAH group provides higher steric hindrance and intramolecular interactions. Accordingly, TA-Phen is difficult to form multiple conformations. In conclusion, the planar and rigid structures of phenanthrene are conducive to inhibiting intramolecular motions and achieving phosphorescent emission of TA-Phen@MF with both a high efficiency and an ultralong lifetime.

Theoretical calculations were conducted to investigate the relationship between the molecular conformation and the photophysical processes. The molecular geometrical structures were extracted based on the information of the single crystal structure and optimized using density functional (DFT) theory at the B3LYP/6-311** level with dispersion correction. Furthermore, their natural transition orbitals (NTOs) and SOC constant were obtained using time-dependent density functional theory (TD-DFT).[59] As TA-Ph and TA-Na exhibit numerous conformations, TA-Ph-1 and TA-Na-2 were used as their examples in the following discussions due to their small geometrical distortion (Fig. 2a), and the details are provided in the ESI (Fig. S12 and S13).† As shown in Fig. 3a, the electronic transition process in the TA molecule is mostly distributed in the whole molecule, dominated by the local excitation (LE) process. Notably, the S_0–S_1 excitation is primarily attributed to the $^1(n, \pi^*)$ transition characteristics according to the contributions of the lone pair electrons of sulfur

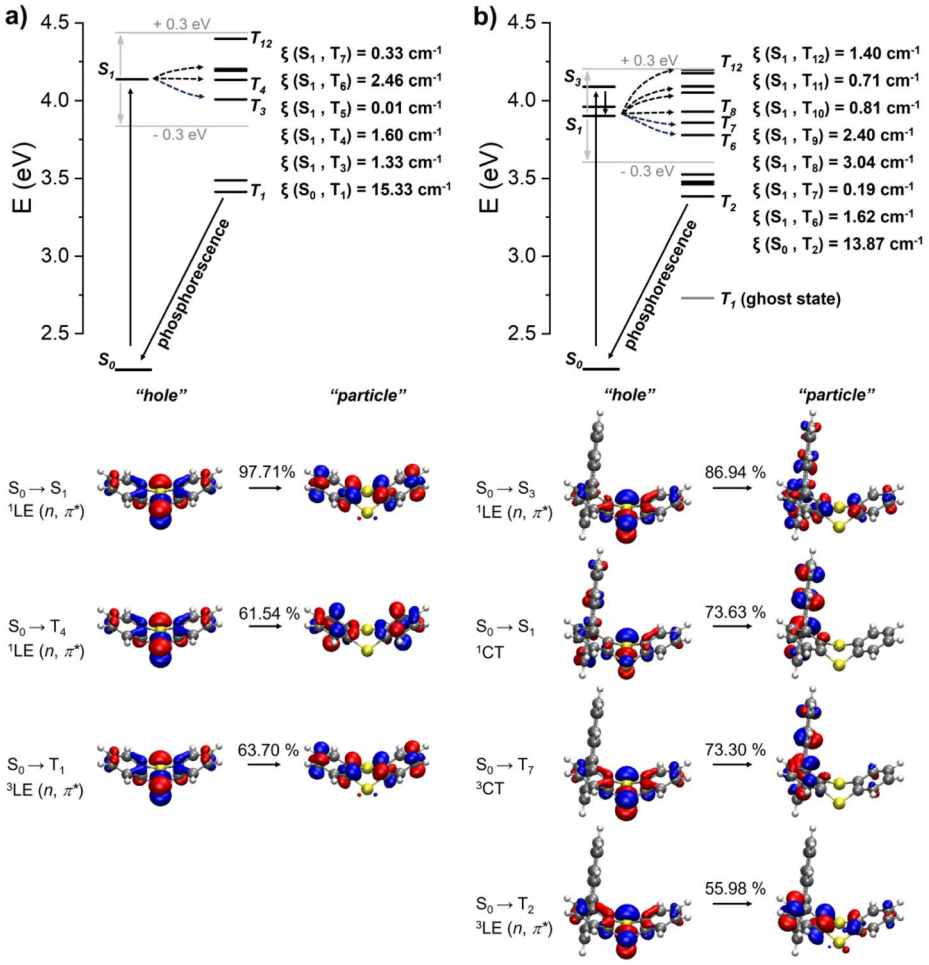

Fig. 3 Diagrams of the calculated energy levels, possible ISC channels, SOC constants between singlet and triplet excited states, the NTO characteristics of singlet and triplet excited states and the corresponding transition contributions of the single molecule of (a) TA and (b) TA-Phen (the ghost state refers to a false CT state with very low energy that is likely to appear when using pure functionals or functionals with a low HF component, see the details in the ESI†).

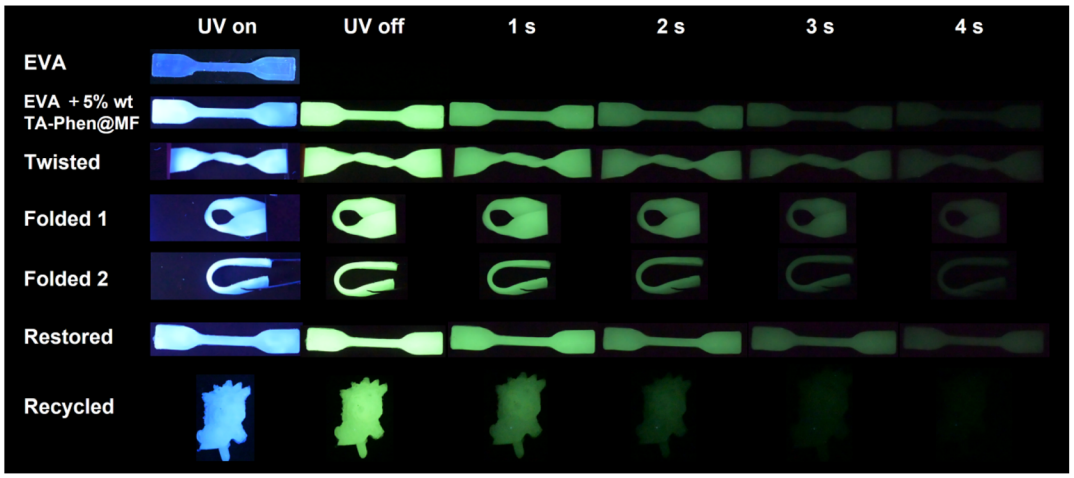

Fig. 4 The RTP afterglow photograph of TA-Phen@MF blending with EVA elastomer materials after twisting, folding and recycling (excitation: 365 nm).

atoms to the electronic processes, whereas the S_0–T_1 excitation is mainly ascribed to the $^3(\pi, \pi^*)$ transition characteristics. When naphthyl and phenanthryl groups are introduced in the molecules, mostly LE excited states are occupied at the higher energy level according to the values of oscillator strength, and the lowest S_1 excitation shows CT characteristics from TA to PAH groups (Fig. 3b, S12a and S12c†). Interestingly, there are some potential ISC channels from S_1 to T_n, where the energy gaps are small enough for the electron transition. The NTO pairs of T_n also show CT characteristics, leading to the considerable SOC constants of $\xi(S_1, T_5) = 2.06\ cm^{-1}$, $\xi(S_1, T_6) = 1.06\ cm^{-1}$, $\xi(S_1, T_7) = 2.00\ cm^{-1}$ and $\xi(S_1, T_8) = 3.32\ cm^{-1}$ for TA-Ph-1 (Fig. S12a†), $\xi(S_1, T_4) = 1.70\ cm^{-1}$, $\xi(S_1, T_5) = 2.51\ cm^{-1}$, $\xi(S_1, T_6) = 3.47\ cm^{-1}$, $\xi(S_1, T_7) = 1.35\ cm^{-1}$, $\xi(S_1, T_8) = 4.65\ cm^{-1}$, $\xi(S_1, T_9) = 2.53\ cm^{-1}$, $\xi(S_1, T_{10}) = 1.52\ cm^{-1}$, and $\xi(S_1, T_{11}) = 5.60\ cm^{-1}$ for TA-Na-2 (Fig. S12c†), and $\xi(S_1, T_6) = 1.62\ cm^{-1}$, $\xi(S_1, T_7) = 0.19\ cm^{-1}$, $\xi(S_1, T_8) = 3.04\ cm^{-1}$, $\xi(S_1, T_9) = 2.40\ cm^{-1}$, $\xi(S_1, T_{10}) = 0.81\ cm^{-1}$, $\xi(S_1, T_{11}) = 0.71\ cm^{-1}$, $\xi(S_1, T_{12}) = 1.40\ cm^{-1}$ f-9*or TA-Phen (Fig. 3b). Meanwhile, the lowest triplet states show a similar LE state with $\xi(S_0, T_1)$ or $\xi(S_0, T_2)$ values of 11.21, 13.76 and 13.87 cm^{-1} for TA-Ph, TA-Na and TA-Phen, respectively. The TA molecule also has a similar $\xi(S_0, T_1)$ value of 15.33 cm^{-1}, indicating analogous phosphorescent emission from the allowed radiative transition of triplet excitons to the ground state (Fig. 3a, b, S12a and S12c†). In conclusion, upon the introduction of extending PAH groups, the CT characters from TA to the PAH group become obvious for the lowest singlet state, especially for TA-Na and TA-Phen. Consequently, TA-Na and TA-Phen undergo a CT intermediate state during the ISC process, which results in an increase of $\tau_{phos.}$ when compared to the TA molecule. Furthermore, the guest molecules in the polymer-based environment were also calculated by introducing the MF fragments (MF*). The NTO analysis and SOC constants were found to be in agreement with the isolated molecule (Fig. S13†). In summary, the introduction of PAH units to TA results in CT features for the electrical excitation, which allows multiple possible ISC processes. The formation of the CT intermediate state leads to an increase of $\tau_{phos.}$. The various metastable conformations of TA-Na, however, indicate that the rotation between TA and naphthyl units could not be disregarded.

Developing persistent RTP materials that can retain their optical properties even after being bent and twisted is highly desirable. Inspired by the efficient RTP and processability properties of TA-Phen@MF, it was blended with elastomer matrices to create twistable materials with stable persistent luminescence properties. TA-Phen@MF was used as the doped MF polymer filler (phosphorescent additive) and blended with the EVA thermoplastic elastomer after crushing. The modified EVA elastomers were formed into dumbbell shapes, as shown in Fig. 4. Obviously, pure EVA exhibited no RTP properties, while the modified EVA (with 5% wt doped MF polymer filler) demonstrated long persistent green luminescence that lasted for more than 4 seconds after the UV light was turned off. The strong persistent green RTP can be clearly observed even after the dumbbell-shaped elastomer was twisted and folded, even in the deformation region. Thanks to the recyclable processing of EVA, the dumbbell samples were then melted and shaped into a small animal, and the persistent green luminescence still lasted over 3 s. It can be seen that these persistent RTP elastomers are mechanically robust, and mechanical deformation only has little effect on their phosphorescence properties. Hence, these colorful polymer-based RTP materials could be facilely prepared into different shapes by hot-pressing, which is favorable for expanding their application scope. The generation of RTP in these elastomers is primarily due to the fact that the MF polymer can effectively immobilize the phosphors due to the presence of hydrogen bond cross-linking between the polymeric chains. These optical elastomers could provide great opportunities for flexible and wearable optoelectronics.

Conclusions

In summary, a synergistic strategy was proposed to promote n–π* transitions, provide CT intermediates and inhibit intramolecular motions to achieve efficient ORTP performance. TA-

based organic afterglow materials with both long lifetimes and high phosphorescence quantum yields were successfully achieved by employing thianthrene derivatives containing different planar and rigid PAHs as guest molecules and embedding them into crosslinked MF polymers, respectively. The TA chromophore promotes n–π* transitions, and PAHs generate CT intermediates and inhibit intramolecular motions, which open ISC channels and facilitate ISC processes. The phosphorescence lifetimes of TA-Na@MF and TA-Phen@MF were about 30-fold that of TA@MF. The phenanthryl group was larger than the naphthyl group, which created steric hindrance and limited rotations. As a result, TA-Phen@MF demonstrated the best RTP performance with an ultralong lifetime of 1006.45 ms and a high phosphorescence quantum yield of 50.31%. Moreover, TA-Phen@MF was blended with EVA to produce stretchable and recyclable persistent RTP elastomers. These results not only provide helpful guidance for creating high-performance polymer-based ORTP materials but also demonstrate a simple and effective strategy for obtaining RTP elastomers.

Data availability

The data supporting this article have been included as part of the ESI.† Data available on request from the authors.

Author contributions

Huiwen Zeng: writing – original draft, conceptualization, methodology and data curation. Hualiu Li: formal analysis and data curation. Peng Zhen: data curation. Jiadong Zhou: supervision and formal analysis. Bingjia Xu: supervision and methodology. Guang Shi: funding acquisition and conceptualization. Yujian Zhang: formal analysis. Zhenguo Chi: formal analysis. Cong Liu: writing – review & editing.

Conflicts of interest

There are no conflicts to declare.

Acknowledgements

This work was supported by the National Natural Science Foundation of China (52473194), the Natural Science Foundation of Guangdong Province of China (2023A1515010915 and 2024A1515010047) and the Shunde Key Technology Project (no. 2030218000189/2030218000191).

Notes and references

1 X. Deng, J. Huang, J. Li, G. Wang and K. Zhang, Sonication-Responsive Organic Afterglow Emulsions, *Adv. Funct. Mater.*, 2023, **33**, 2214960.

2 D. Guo, W. Wang, K. Zhang, J. Chen, Y. Wang, T. Wang, W. Hou, Z. Zhang, H. Huang, Z. Chi and Z. Yang, Visible-light-excited robust room-temperature phosphorescence of dimeric single-component luminophores in the amorphous state, *Nat. Commun.*, 2024, **15**, 3598.

3 J. Shi, Y. Zhou, W. Wang, Z. Yang, P. Zhang and G. Liang, Scalable fabrication of red Room-Temperature phosphorescent materials through molecular doping strategy for versatile applications, *Chem. Eng. J.*, 2024, **492**, 152419.

4 D. Wang, J. Gong, Y. Xiong, H. Wu, Z. Zhao, D. Wang and B. Z. Tang, Achieving Color-Tunable and Time-Dependent Organic Long Persistent Luminescence via Phosphorescence Energy Transfer for Advanced Anti-Counterfeiting, *Adv. Funct. Mater.*, 2023, **33**, 2208895.

5 Y. Yang, Y. Liang, Y. Zheng, J.-A. Li, S. Wu, H. Zhang, T. Huang, S. Luo, C. Liu, G. Shi, F. Sun, Z. Chi and B. Xu, Efficient and Color-Tunable Dual-Mode Afterglow from Large-Area and Flexible Polymer-Based Transparent Films for Anti-Counterfeiting and Information Encryption, *Angew. Chem., Int. Ed.*, 2022, **61**, e202201820.

6 Y. Yang, A. Li, Y. Yang, J. Wang, Y. Chen, K. Yang, B. Z. Tang and Z. Li, Multi-stimulus Room Temperature Phosphorescent Polymers Sensitive to Light and Acid cyclically with Energy Transfer, *Angew. Chem., Int. Ed.*, 2023, **62**, e202308848.

7 X. Zhang, J. Liu, B. Chen, X. He, X. Li, P. Wei, P. F. Gao, G. Zhang, J. W. Y. Lam and B. Z. Tang, Highly efficient and persistent room temperature phosphorescence from cluster exciton enables ultrasensitive off-on VOC sensing, *Matter*, 2022, **5**, 3499–3512.

8 X. Luo, L. Chen, B. Liu, Z. Yang, L. Wei, Z. Yuan, Y. Wen, Y. Mu, Y. Huo, H.-L. Zhang and S. Ji, Water-enhanced high-efficiency persistent room-temperature phosphorescence materials for temperature sensing via crystalline transformation, *J. Mater. Chem. C*, 2022, **10**, 13210–13216.

9 Z. Lü, Q. Gao, M. Shi, Z. Su, G. Chen, H. Qi, B. Lü and F. Peng, Colorful Room-Temperature Phosphorescence Including White Afterglow from Mechanical Robust Transparent Wood for Time Delay Lighting, *Small Struct.*, 2024, **5**, 2300567.

10 K. Chen, Y. Xiong, D. Wang, Y. Pan, Z. Zhao, D. Wang and B. Z. Tang, A Facile Strategy for Achieving Polymeric Afterglow Materials with Wide Color-Tunability and Persistent Near-Infrared Luminescence, *Adv. Funct. Mater.*, 2024, **34**, 2312883.

11 Y. Zhang, Q. Sun, L. Yue, Y. Wang, S. Cui, H. Zhang, S. Xue and W. Yang, Room Temperature Phosphorescent (RTP) Thermoplastic Elastomers with Dual and Variable RTP Emission, Photo-Patterning Memory Effect, and Dynamic Deformation RTP Response, *Adv. Sci.*, 2022, **9**, 2103402.

12 Y. Gao, Q. Zhang, F. Wang and P. Sun, Wide-range tunable phosphorescence emission in cellulose-based materials enabled by complementary-color phosphors, *Chem. Eng. J.*, 2023, **471**, 144665.

13 X. Yang, S. Wang, K. Sun, H. Liu, M. Ma, S.-T. Zhang and B. Yang, A Heavy-atom-free Molecular Motif Based on Symmetric Bird-like Structured Tetraphenylenes with Room-Temperature Phosphorescence (RTP) Afterglow over 8 s, *Angew. Chem., Int. Ed.*, 2023, **62**, e202306475.

14 D.-X. Ma, Z.-Q. Li, K. Tang, Z.-L. Gong, J.-Y. Shao and Y.-W. Zhong, Nylons with Highly-Bright and Ultralong Organic Room-Temperature Phosphorescence, *Nat. Commun.*, 2024, **15**, 4402.

15 Y. He, J. Wang, Q. Li, S. Qu, C. Zhou, C. Yin, H. Ma, H. Shi, Z. Meng and Z. An, Highly Efficient Room-Temperature Phosphorescence Promoted via Intramolecular-Space Heavy-Atom Effect, *Adv. Opt. Mater.*, 2023, **11**, 2201641.

16 H. Zhang, S. Wu, Y. Liang, Z. Zhang, H. Wei, Q. Yang, P. Hu, C. Liu, Z. Yang, C. Zheng, G. Shi, Z. Chi and B. Xu, Enabling efficient and ultralong room-temperature phosphorescence from organic luminogens by locking the molecular conformation in polymer matrix, *Chem. Eng. J.*, 2024, **497**, 154949.

17 T.-F. He, A.-M. Ren, Y.-N. Chen, X.-L. Hao, L. Shen, B.-H. Zhang, T.-S. Wu, H.-X. Zhang and L.-Y. Zou, Molecular-Level Insight of Cu(I) Complexes with the 7,8-Bis(diphenylphosphino)-7,8-dicarba-nido-undecaborate Ligand as a Thermally Activated Delayed Fluorescence Emitter: Luminescent Mechanism and Design Strategy, *Inorg. Chem.*, 2020, **59**, 12039–12053.

18 A. Abe, K. Goushi, M. Mamada and C. Adachi, Organic Binary and Ternary Cocrystal Engineering Based on Halogen Bonding Aimed at Room-Temperature Phosphorescence, *Adv. Mater.*, 2024, **36**, e2211160.

19 J. Chen, Y. Zhang, S. Zhang, G. Liu, Q. Sun, S. Xue and W. Yang, Two-Phase Rubber–Plastic Matrices' Stabilization of Organic Room-Temperature Phosphorescence Afterglows Better than Plastic Matrix, *Small Struct.*, 2023, **4**, 2300101.

20 S. Zhang, W. Yao, A. Lv, K. Liu, Y. Zhang, C. Zhou, H. Ma, H. Shi and Z. An, Achieving highly efficient long-wavelength phosphorescence emission of large singlet-triplet energy gap materials by host-guest doping, *Sci. China Chem.*, 2024, **67**, 1922–1928.

21 Z. Guan, Z. Tang, J. Deng, Y. Zheng, H. Li and X. Liu, Multi-Color Pure Organic Room Temperature Phosphorescent Materials with Long Lifetime and High Efficiency, *Adv. Funct. Mater.*, 2024, **34**, 2310198.

22 J. Xiao, J. Deng, Y. Bai, H. Liu, L. Yu and H. Wang, Persistent Room-Temperature Phosphorescent Triazole Derivatives with High Quantum Yields and Long Lifetimes, *Adv. Opt. Mater.*, 2024, **12**, 2301978.

23 H. Ma, Q. Peng, Z. An, W. Huang and Z. Shuai, Efficient and Long-Lived Room-Temperature Organic Phosphorescence: Theoretical Descriptors for Molecular Designs, *J. Am. Chem. Soc.*, 2019, **141**, 1010–1015.

24 S. Zhao, Z. Yang, X. Zhang, H. Liu, Y. Lv, S. Wang, Z. Yang, S. T. Zhang and B. Yang, A functional unit combination strategy for enhancing red room-temperature phosphorescence, *Chem. Sci.*, 2023, **14**, 9733–9743.

25 H. Ma, L. Fu, X. Yao, X. Jiang, K. Lv, Q. Ma, H. Shi, Z. An and W. Huang, Boosting organic phosphorescence in adaptive host-guest materials by hyperconjugation, *Nat. Commun.*, 2024, **15**, 3660.

26 G. Pan, Z. Yang, H. Liu, Y. Wen, X. Zhang, Y. Shen, C. Zhou, S.-T. Zhang and B. Yang, Folding-Induced Spin–Orbit Coupling Enhancement for Efficient Pure Organic Room-Temperature Phosphorescence, *J. Phys. Chem. Lett.*, 2022, **13**, 1563–1570.

27 L. Volyniuk, D. Gudeika, A. A. Panchenko, B. F. Minaev, M. Mahmoudi, J. Simokaitiene, A. Bucinskas, D. Volyniuk and J. V. Grazulevicius, Single-Molecular White Emission of Organic Thianthrene-Based Luminophores Exhibiting Efficient Fluorescence and Room Temperature Phosphorescence Induced by Halogen Atoms, *ACS Sustainable Chem. Eng.*, 2023, **11**, 16914–16925.

28 H. Wang, F. Hao, Z. Ba, Y. Xiao and T. Yu, Realizing mechano-tunable dual emission in a twisted thianthrene derivative, *Dyes Pigm.*, 2024, **223**, 111932.

29 M. Liu, Z. Yang, Z. Feng, N. Zhao, R. Bian, J. Wu, Q. Yang, S. Zhao, H. Liu and B. Yang, Combining Functional Units to Design Organic Materials with Dynamic Room-Temperature Phosphorescence under Continuous Ultraviolet Irradiation, *Molecules*, 2024, **29**, 2621.

30 H. Liu, G. Pan, Z. Yang, Y. Wen, X. Zhang, S.-T. Zhang, W. Li and B. Yang, Dual-Emission of Fluorescence and Room-Temperature Phosphorescence for Ratiometric and Colorimetric Oxygen Sensing and Detection Based on Dispersion of Pure Organic Thianthrene Dimer in Polymer Host, *Adv. Opt. Mater.*, 2022, **10**, 2102814.

31 Z. Yang, H. Liu, X. Zhang, Y. Lv, Z. Fu, S. Zhao, M. Liu, S.-T. Zhang and B. Yang, Photo-Responsive Dynamic Organic Room-Temperature Phosphorescence Materials Based on a Functional Unit Combination Strategy, *Adv. Mater.*, 2024, **36**, 2306784.

32 N. Li, Y. Wang and Z. Li, Photo-induced room temperature phosphorescence and thermally activated photochromism based on thianthrene derivatives, *J. Mater. Chem. C*, 2024, **12**, 12045–12053.

33 M. Singh, K. Shen, W. Ye, Y. Gao, A. Lv, K. Liu, H. Ma, Z. Meng, H. Shi and Z. An, Achieving High-Temperature Phosphorescence by Organic Cocrystal Engineering, *Angew. Chem., Int. Ed.*, 2024, **63**, e202319694.

34 H. Deng, G. Li, H. Xie, Z. Yang, Z. Mao, J. Zhao, Z. Yang, Y. Zhang and Z. Chi, Dynamic Ultra-long Room Temperature Phosphorescence Enabled by Amorphous Molecular "Triplet Exciton Pump" for Encryption with Temporospatial Resolution, *Angew. Chem., Int. Ed.*, 2024, **63**, e202317631.

35 A. Lv, W. Gong, K. Lv, Q. Ma, Z. An and H. Ma, Molecular Insight into the Water-Induced Enhancement of Room-Temperature Phosphorescence in Organic Aggregates, *Adv. Opt. Mater.*, 2024, **12**, 2301937.

36 F. Nie, B. Zhou and D. Yan, Ultralong room temperature phosphorescence and reversible mechanochromic luminescence in ionic crystals with structural isomerism, *Chem. Eng. J.*, 2023, **453**, 139806.

37 A. Huang, Y. Fan, K. Wang, Z. Wang, X. Wang, K. Chang, Y. Gao, M. Chen, Q. Li and Z. Li, Organic Persistent RTP Crystals: From Brittle to Flexible by Tunable Self-Partitioned Molecular Packing, *Adv. Mater.*, 2023, e2209166, DOI: **10.1002/adma.202209166**.

38 Y. Chen, A. Li, X. Li, L. Tu, Y. Xie, S. Xu and Z. Li, Multi-Stimuli-Responsive Amphiphilic Pyridinium Salt and Its Application in the Visualization of Level 3 Details in Latent Fingerprints, *Adv. Mater.*, 2023, **35**, 2211917.

39 Z. Deng, J. Zhang, J. Zhou, W. Shen, Y. Zuo, J. Wang, S. Yang, J. Liu, Y. Chen, C.-C. Chen, G. Jia, P. Alam, J. W. Y. Lam and B. Z. Tang, Dynamic Transition between Monomer and Excimer Phosphorescence in Organic Near-Infrared Phosphorescent Crystals, *Adv. Mater.*, 2024, **36**, 2311384.

40 F. Xiao, H. Gao, Y. Lei, W. Dai, M. Liu, X. Zheng, Z. Cai, X. Huang, H. Wu and D. Ding, Guest-host doped strategy for constructing ultralong-lifetime near-infrared organic phosphorescence materials for bioimaging, *Nat. Commun.*, 2022, **13**, 186.

41 D. Li, Z. Liu, M. Fang, J. Yang, B. Z. Tang and Z. Li, Ultralong Room-Temperature Phosphorescence with Second-level Lifetime in Water Based on Cyclodextrin Supramolecular Assembly, *ACS Nano*, 2023, **17**, 12895–12902.

42 L. Zhou, J. Song, Z. He, Y. Liu, P. Jiang, T. Li and X. Ma, Achieving Efficient Dark Blue Room-Temperature Phosphorescence with Ultra-Wide Range Tunable-Lifetime, *Angew. Chem., Int. Ed.*, 2024, **63**, e202403773.

43 X. Zhang, Y. Liu, L. Bu, J. Bai, Z. Li, Z. Ma, M. Chen, Y. Guan and Z. Ma, Site Effect of Electron Acceptors on Ultralong Organic Room-Temperature Phosphorescence, *ACS Appl. Mater. Interfaces*, 2024, **16**, 59004–59014.

44 J. Wang, Y. Yang, K. Li, L. Zhang and Z. Li, Purely Organic Fluorescence Afterglow: Visible-Light-Excitation, Inherent Mechanism, Tunable Color, and Practical Applications with Very Low Cost, *Angew. Chem., Int. Ed.*, 2023, **62**, e202304020.

45 Y. Xu, Y. Zhu, L. Kong, S. Sun, F. Li, F. Tao, L. Wang and G. Li, Efficient ultralong and color-tunable room-temperature phosphorescence from polyacrylamide platform by introducing sulfanilic acid, *Chem. Eng. J.*, 2023, **453**, 139753.

46 N. Gan, X. Zou, Z. Qian, A. Lv, L. Wang, H. Ma, H.-J. Qian, L. Gu, Z. An and W. Huang, Stretchable phosphorescent polymers by multiphase engineering, *Nat. Commun.*, 2024, **15**, 4113.

47 Y. Miao, F. Lin, D. Guo, J. Chen, K. Zhang, T. Wu, H. Huang, Z. Chi and Z. Yang, Stable and ultralong room-temperature phosphorescent copolymers with excellent adhesion, resistance, and toughness, *Sci. Adv.*, 2024, **10**, eadk3354.

48 Y.-Y. Hu, X.-Y. Dai, X. Dong, M. Huo and Y. Liu, Generation of Tunable Ultrastrong White-Light Emission by Activation of a Solid Supramolecule through Bromonaphthylpyridinium Polymerization, *Angew. Chem., Int. Ed.*, 2022, **61**, e202213097.

49 Q. Zhang, P. Hu, C. Han, Z. Mao, R. Chen, Z. Liang, W. Cai, L. Wang, Z. Yang, C. Zheng, C. Liu, G. Shi and B. Xu, Elucidating the Crystallization-Caused Phosphorescence Quenching Mechanism to Achieve Efficient Photoactivated Persistent Luminescence for High-Quality Light Printing, *Adv. Opt. Mater.*, 2024, **12**, 2400642.

50 S. Wu, H. Zhang, Z. Mao, Y. Liang, J.-A. Li, P. Hu, Q. Zhang, C. Liu, S. Luo, Y. Wang, G. Shi and B. Xu, Achieving Stable and Switchable Ultralong Room-Temperature Phosphorescence from Polymer-Based Luminescent Materials with Three-Dimensional Covalent Networks for Light-Manipulated Anticounterfeiting, *ACS Appl. Mater. Interfaces*, 2023, **15**, 39896–39904.

51 Y. Zhang, J. Chen, Q. Sun, H. Zhang, S. Xue and W. Yang, In-situ grafting N-arylcarbazoles enables more ultra-long room temperature phosphorescence polymers, *Chem. Eng. J.*, 2023, **452**, 139385.

52 D. Li, Y. Yang, J. Yang, M. Fang, B. Z. Tang and Z. Li, Completely aqueous processable stimulus responsive organic room temperature phosphorescence materials with tunable afterglow color, *Nat. Commun.*, 2022, **13**, 347.

53 J.-A. Li, L. Zhang, C. Wu, Z. Huang, S. Li, H. Zhang, Q. Yang, Z. Mao, S. Luo, C. Liu, G. Shi and B. Xu, Switchable and Highly Robust Ultralong Room-Temperature Phosphorescence from Polymer-Based Transparent Films with Three-Dimensional Covalent Networks for Erasable Light Printing, *Angew. Chem., Int. Ed.*, 2023, **62**, e202217284.

54 J. Liang, J. Yang, Y. Wang, M. Shan, Z. Liu, J. Ren, M. Fang and Z. Li, Efficient photo-induced RTP materials based on phenothiazine and polycyclic aromatic hydrocarbons: Tunable emission color and thermal stimulus response, *Sci. China Mater.*, 2024, **67**, 2778–2788.

55 Y. Liang, P. Hu, H. Zhang, Q. Yang, H. Wei, R. Chen, J. Yu, C. Liu, Y. Wang, S. Luo, G. Shi, Z. Chi and B. Xu, Enabling Highly Robust Full-Color Ultralong Room-Temperature Phosphorescence and Stable White Organic Afterglow from Polycyclic Aromatic Hydrocarbons, *Angew. Chem., Int. Ed.*, 2024, **63**, e202318516.

56 X. Meng, Q. Hu, X. Wang, T. Ma, W. Liu, X. Zhu and C. Ye, Ultralong room-temperature phosphorescence from polycyclic aromatic hydrocarbons by accelerating intersystem crossing within a rigid polymer network, *J. Mater. Chem. C*, 2022, **10**, 17620–17627.

57 X. Zheng, Q. Han, Q. Lin, C. Li, J. Jiang, Q. Guo, X. Ye, W. Z. Yuan, Y. Liu and X. Tao, A processable, scalable, and stable full-color ultralong afterglow system based on heteroatom-free hydrocarbon doped polymers, *Mater. Horiz.*, 2023, **10**, 197–208.

58 T. Lu and Q. Chen, Interaction Region Indicator: A Simple Real Space Function Clearly Revealing Both Chemical Bonds and Weak Interactions, *Chem.: Methods*, 2021, **1**, 231–239.

59 T. Lu and F. Chen, Multiwfn: A multifunctional wavefunction analyzer, *J. Comput. Chem.*, 2012, **33**, 580–592.